ELSEVIER

Seminars in
ULTRASOUND
CT and MRI

FDG-PET Imaging of Salivary Gland Tumors

Cody R. Larson, MD, and Richard H. Wiggins, MD

The salivary glands are host to a variety of benign and malignant tumors, as well as tumor-like conditions. Due to the variable FDG avidity of these lesions on positron emission tomography (PET) imaging, as well as the complex embryology and physiology that affect normal FDG uptake, FDG PET imaging of salivary gland pathology can prove challenging for head and neck imagers. We provide a practical guide for PET imaging of salivary gland tumors, detailing important additional diagnostic considerations, such as perineural tumor spread and intraparotid nodal metastases that are unique subsets related to salivary gland malignancy.
Semin Ultrasound CT MRI 40:391-399

Introduction

The salivary glands are host to a variety of benign and malignant pathologies, as well as several congenital and acquired conditions with associated mass-like lesions. Salivary gland malignancies are actually relatively rare, representing less than 10% of all head and neck tumors. Determination of benignity cannot always be ascertained based on imaging features alone; however, the use of modern imaging techniques including computed tomography (CT), magnetic resonance imaging (MRI), positron emission tomography (PET), PET/CT, and PET/MR can provide increased diagnostic information when faced with a potential salivary gland mass. Although there is limited published data on 18F-labeled fluoro-2-deoxyglucose-PET (FDG-PET) imaging of salivary gland tumors, a few general rules can be applied to assist with evaluation.

When evaluating a salivary gland mass on FDG-PET imaging, several questions should be posed for appropriate evaluation:

(1) Does the patient have a known malignancy (ie, is this an incidentally discovered lesion)?
(2) What are the FDG-PET characteristics of the mass relative to normal salivary gland parenchyma?
(3) Is the pathology centered within the parotid gland? Or is the lesion within one of the smaller salivary glands?

The critical evaluation of complex salivary gland lesions can help to differentiate malignancies from other pathologies that may be more common in certain salivary glands. Because of this complicated imaging evaluation, it is important to understand both the differences in the embryologic development of these salivary glands, and also to understand how tumors and other masses can be distinguished on imaging. This chapter will briefly review the salivary gland embryology and then review the tumors and other mass-like lesions that occur within these tissues, focusing on the imaging appearance and utilization of FDG-PET to distinguish tumors from other mass-like lesions, as well as primary and metastatic disease.[1-3]

While FDG-PET imaging may not appear initially useful in distinguishing some salivary gland pathologies (Fig. 1), it can be critical in evaluating both the post-therapy cases (Fig. 2) and in the work-up of possible distant disease (Fig. 3).

Salivary Gland Development

The embryologic development of the parotid glands allows some unique considerations when a parotid mass is encountered. The parotid gland anlagen develop early in embryogenesis (around 4-6 weeks gestation) and continues until fascial encasement of the glandular tissue by the deep cervical fascia after 12 weeks. Through this developmental process, the parotid glands migrate posteriorly from the initial anlagen location within the anterior cheek over the masseter muscles and toward the angle of the mandible. At 6-8 weeks gestation, during this period of parotid formation, the cervical lymphatic tissues undergo simultaneous development alongside the parotid anlagen near the angle of the mandible. This relatively early development and late encapsulation results in the inclusion of vascular, peripheral nervous, and lymphatic tissues within the parenchyma of the parotid glands, predisposing them to disease processes not seen within the

University of Utah Health Sciences Center, Salt Lake City, UT.
Disclosure: The authors report no disclosures, financial or otherwise.
Address reprint requests to Richard H. Wiggins, MD, University of Utah Health Sciences Center, Salt Lake City, UT. E-mail: Richard.Wiggins@hsc.utah.edu

https://doi.org/10.1053/j.sult.2019.07.003

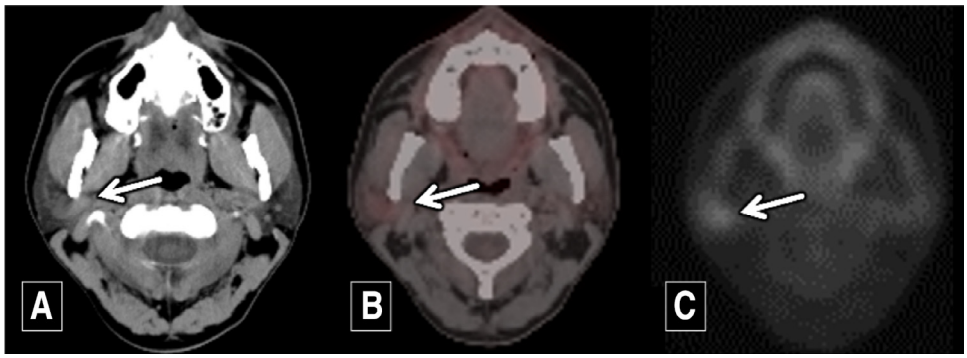

Figure 1 A 40-year-old man with a subtle right parotid mass found to be a mucoepidermoid carcinoma on biopsy. Axial standard algorithm CT (A) shows a subtle mass (arrow) within the deep lobe of the right parotid with density similar to skeletal muscle. Axial fused FDG-PET/CT (B) shows slight increased uptake in this lesion (arrow), which is more prominent on the axial FDG-PET (C) image (arrow).

other salivary glands, including pathologies of lymphatic origin, neurogenic origin, and perineural spread of disease.

Contrary to parotid gland formation, the development of the submandibular, sublingual, minor salivary, and lacrimal glands is a much simpler process. These glands do not undergo significant spatial migration. The fascial encasement of these glandular tissues tends to be much more rapid, preventing the inclusion of simultaneously forming tissues, as is seen with the parotid glands.

Developmental Lesions

The parotid glands can host a variety of developmental lesions that may mimic tumors on FDG-PET imaging. As the glandular tissue migrates from its origin near the buccal mucosa to the region of the mandibular angle, the parotid parenchyma overlying the masseter muscle regresses, leaving behind the parotid duct. Incomplete involution of this glandular tissue may result in small nodules of parotid parenchyma along the course of the parotid duct, mimicking a mass within the parotid and/or masticator spaces on clinical examination. The parotid parenchyma may also be entirely found superficial to the masseter muscle, anterior to the expected parotid bed location.

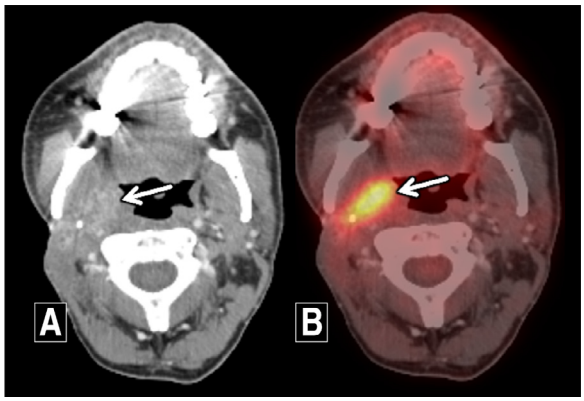

Figure 2 Parotid mucoepidermoid carcinoma, post-treatment surveillance. Axial postcontrasted CT image (A) through the level of the mandible posterior body shows abnormal heterogeneous density (arrow) within the deep lobe of the right parotid near the site of the original lesion in Figure 1, greater than 5 years after the initial surgery and radiation therapy. Axial fused FDG-PET/CT image through the same level (B) shows significant increased uptake consistent with recurrence of mucoepidermoid carcinoma (arrow).

Anomalous formation of the paired first and second branchial cleft/pouch can leave residual cysts within the parotid glands, mimicking a primary parotid mass. Less commonly, fistulae and/or sinus tracts associated with branchial malformation results in abnormal intraparotid anatomy. The inclusion of malformed mesenchymal tissues within the salivary glands can result in a variety of benign congenital masses, including lipomas and low-flow (eg, venolymphatic) vascular malformations, which can also mimic tumors on imaging.

Encephalotrigeminal angiomatosis (Sturge-Weber syndrome), one of the congenital phakomatoses, results from malformation of embryologic capillaries and venous structures with subsequent abnormal development of the cerebral and facial soft tissues. The findings in this syndrome are typically unilateral and may include hemihypertrophy of the salivary glands without focal mass development.

Lymphatic Metastases and Primary Lymphatic Lesions

Unique to the parotid gland, intraglandular lymphatic tissue predisposes these salivary glands to pathologies not seen in the other salivary glands. Up to 10% of patients with HIV will develop lymphatic abnormalities within the parotid glands, including lymphadenopathy and lymphoepithelial cysts. The cervical lymphatic tissue contained within the parotid glands serves as the primary drainage pathway for the anterior parietooccipital scalp, cheek, buccal mucosa, pinna, and parotid tissue. Therefore, intranodal metastasis from primary skin cancer (typically squamous cell carcinoma, basal cell carcinoma, or melanoma) may be seen within the parotid glands, and accounts for up to 10% of all salivary gland malignancy[1,2,4] (Fig. 4). Less commonly, metastases from distant primary neoplasms including thyroid, breast, and lung malignancy may

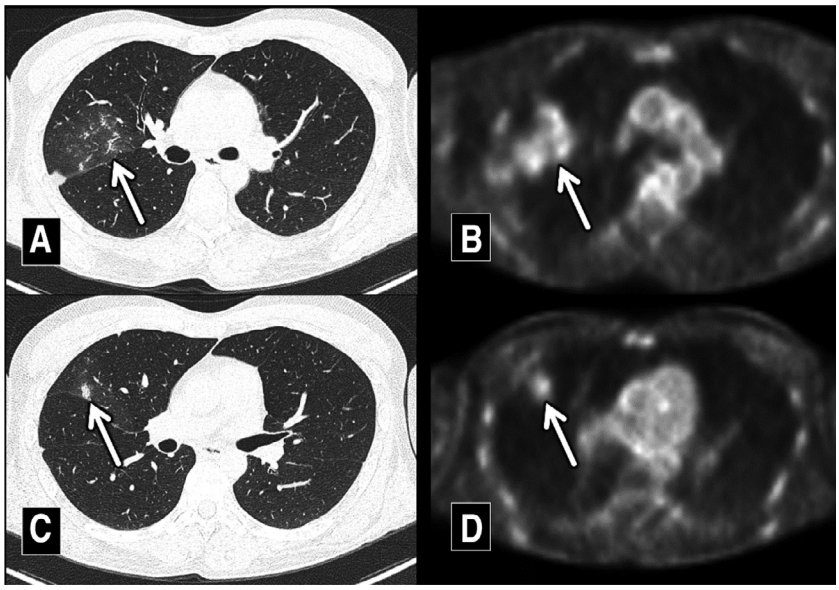

Figure 3 Parotid mucoepidermoid carcinoma, post-treatment surveillance. Axial lung algorithm CT images (A and C) and correlating axial FDG-PET images (B and D) demonstrate distant metastatic disease (arrows) found over 5 years later in the same patient as Figures 1 and 2.

present as intraparotid lymphadenopathy. FDG-PET imaging can assist not only in imaging metastatic disease from a salivary gland malignancy,[3] but can also be utilized in the workup evaluation of distant metastatic disease to a salivary gland.[4] The aggressive nature of the underlying metastatic disease may result in varying appearances, from focal metastatic adenopathy to ill-defined infiltrative appearing processes. FDG-PET imaging has also been described in the literature for further differentiation of a synchronous unrelated salivary gland lesion found during a malignancy work-up.[5] (Fig. 5).

Primary Salivary Gland Malignancy

As detailed previously, the prevalence of salivary gland neoplasm is roughly related to the salivary gland size, in decreasing order: parotid glands (most common), submandibular glands, minor salivary glands, and sublingual glands (least common) (Fig. 6). Accounting for the bulk of all salivary gland masses, benign primary parotid gland neoplasms include pleomorphic adenoma (benign mixed tumor) (69%), papillary cystadenoma lymphomatosum (or Warthin tumor, if you like to name stuff after dead people) (25%), oncocytoma (1%), and other various benign tumors (5%). Malignant parotid gland neoplasms include mucoepidermoid carcinoma (29%), adenocarcinoma not otherwise specified (22%), acinar cell carcinoma (16%), adenoid cystic carcinoma (14%), carcinoma ex pleomorphic adenoma (5%), and other malignant neoplasms (14%).[1,4,6] In these complex cases, FDG-PET imaging can be extremely helpful in the work-up of possible distant metastatic disease (Fig. 7).

A potential dilemma in FDG-PET imaging of the head and neck is the presence of a salivary gland mass which may or

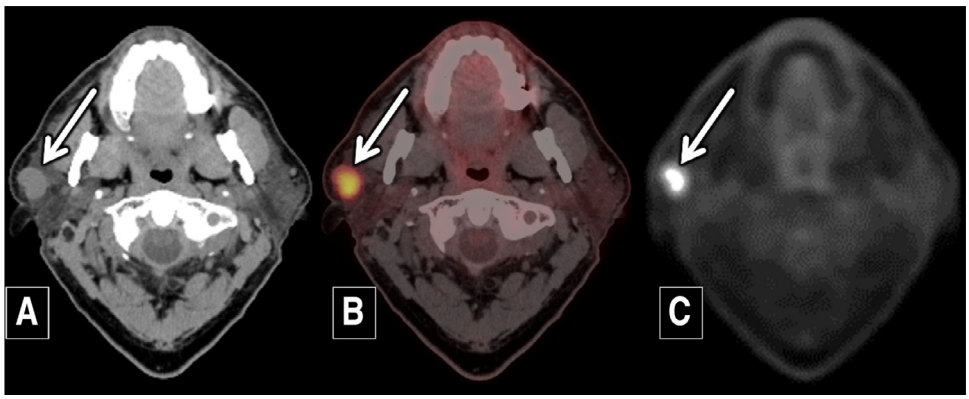

Figure 4 FDG-PET/CT for staging of melanoma of unknown primary. A 55-year-old man with an axial standard algorithm CT image (A), and correlating axial fused FDG-PET/CT image (B), and axial FDG-PET image (C) show a dense right superficial parotid mass (A, arrow) with increased FDG uptake (B and C, arrows), which was found on biopsy to be a metastatic melanoma focus of unknown primary.

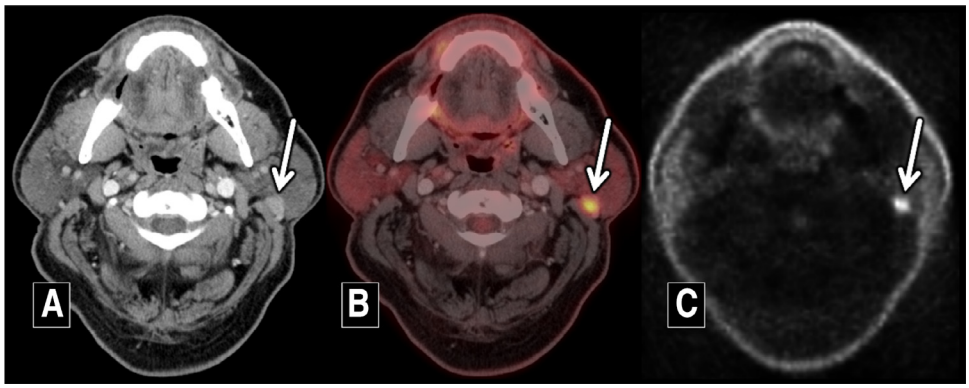

Figure 5 A 65-year-old man with a small mass within the superficial left parotid (arrows) on axial postcontrasted standard algorithm CT (A) with correlating fused axial FDG-PET/CT (B) and axial FDG-PET (C). This patient was being evaluated for an unrelated upper aerodigestive tract primary and this lesion was found incidentally. Subsequent biopsy found papillary cystadenoma lymphomatosum (Warthin tumor), a benign tumor that may show marked FDG avidity.

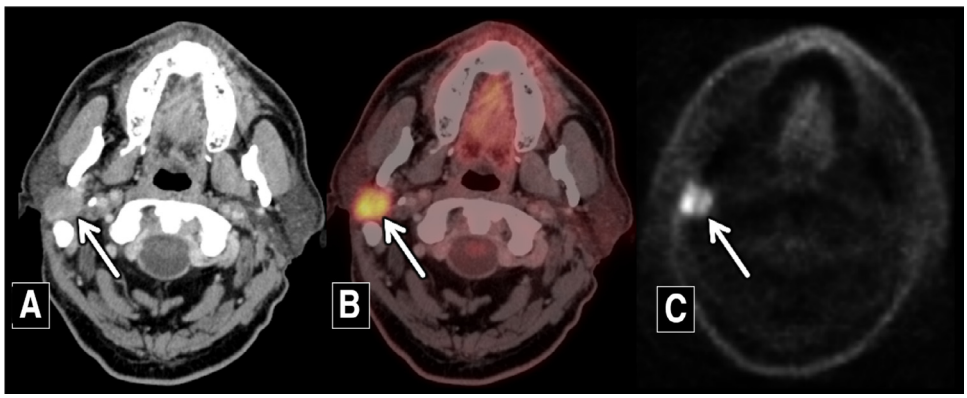

Figure 6 A 70-year-old woman with a right parotid mass (arrows) and unilateral facial palsy on clinical evaluation. The mass is nicely demonstrated on axial postcontrasted standard algorithm CT (A, arrow), and the correlating axial FDG-PET/CT (B), and axial FDG-PET (C) show increased FDG uptake. Biopsy demonstrated salivary duct carcinoma.

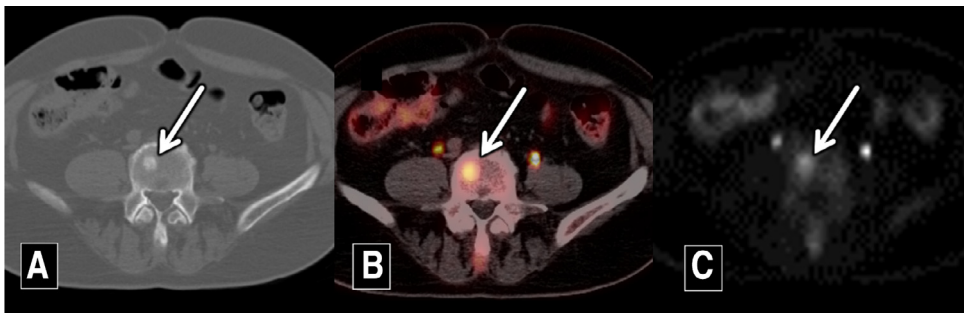

Figure 7 During the workup for the parotid salivary duct carcinoma in Figure 6, the same patient was found to have an unsuspected metastatic focus (arrows) in the lumbar spine. Axial bone algorithm CT (A) and the correlating axial fused FDG-PET/CT (B) and axial FDG-PET (C) images readily identify the osseous metastatic focus.

may not be related to the patient's known malignancy, the so-called "incidentaloma." Several studies have evaluated parotid gland incidentalomas with FDG uptake greater than the surrounding parotid tissue with conflicting conclusions. The presence of malignancy in these masses has been found to range from 4% to 50%.[7,8] Despite this incongruity, there seems to be agreeance that FDG-avid parotid gland masses in patients with known history of lymphoma or melanoma should be considered highly suspicious for metastatic disease.[1,4,6]

It is critical for interpreting radiologists to remember that FDG avidity is simply a marker of cellular glucose metabolism. While many aggressive neoplastic and non-neoplastic processes may demonstrate hypermetabolism with FDG-PET, Warthin tumors are a very common benign salivary neoplasm which demonstrates increased FDG uptake.[5] Conversely, low-grade malignant tumors may have relatively low glucose metabolism and appear "cold" (hypometabolic) on FDG-PET imaging. Despite its limitations in situations such as these, the use of FDG-PET/CT can assist greatly with

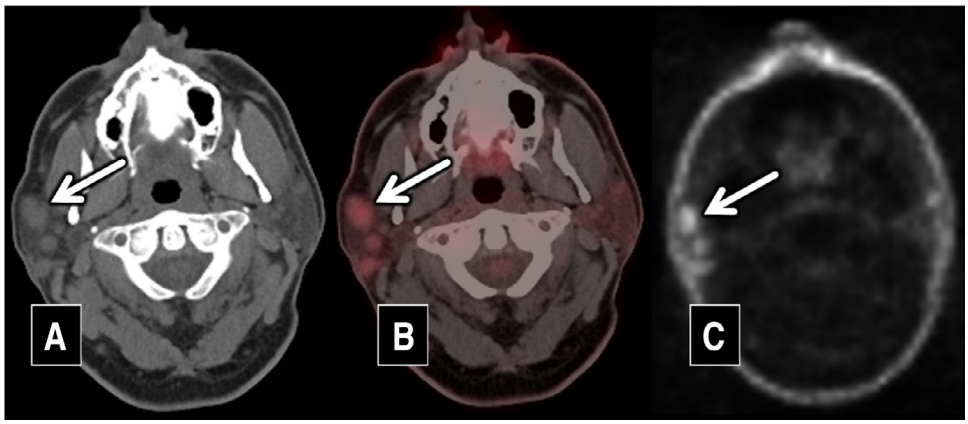

Figure 8 A 55-year-old man with a history of lymphoma found to have multiple masses within the bilateral parotid glands on axial standard algorithm CT (A, arrow), with correlating increased FDG uptake on axial fused FDG-PET/CT (B, arrow) and axial FDG-PET (C, arrow).

known hypermetabolic neoplasms when evaluating the extent of metastatic disease for patient staging and treatment planning[6,7] (Fig. 8).

Given their relatively large size, the parotid glands account for most salivary gland tumors, both benign and malignant. Approximately 70% of all salivary gland tumors arise from the parotid glands. The presence of nodes within the parotid can also be confusing with adjacent aggressive pathologies (Figs. 9 and 10). The relative frequency of salivary gland tumors subsequently decreases based on gland size, as follows: submandibular glands (most common), sublingual glands, and finally, minor salivary glands (least common). In

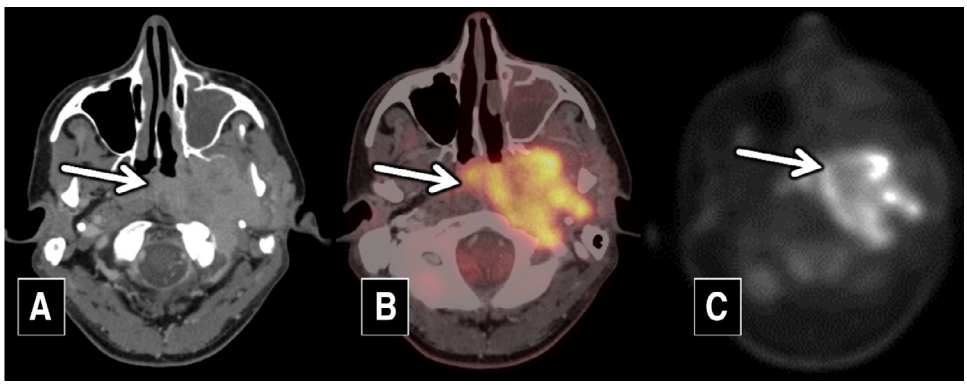

Figure 9 A 25-year-old man with nasopharyngeal carcinoma demonstrating aggressive lateral spread (arrows) toward the deep lobe of the left parotid seen on axial postcontrasted standard algorithm CT (A, arrow), correlating axial fused FDG-PET/CT (B, arrow), and axial PET (C, arrow).

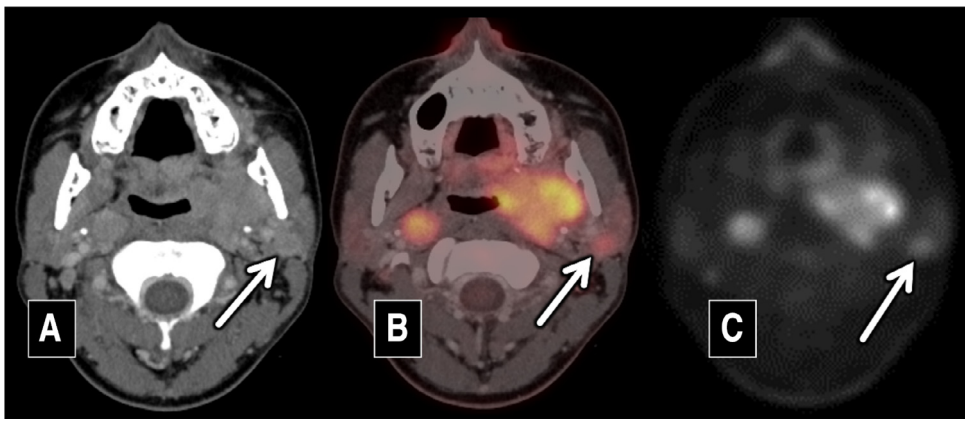

Figure 10 Same patient as in Figure 9 with nasopharyngeal carcinoma was found to have a contralateral right sided retropharyngeal pathologic lymph node. Note an ipsilateral left-sided pathologic intraparotid lymph node found on axial postcontrasted CT (A, arrow), correlating axial fused FDG-PET/CT (B, arrow), and axial PET (C, arrow).

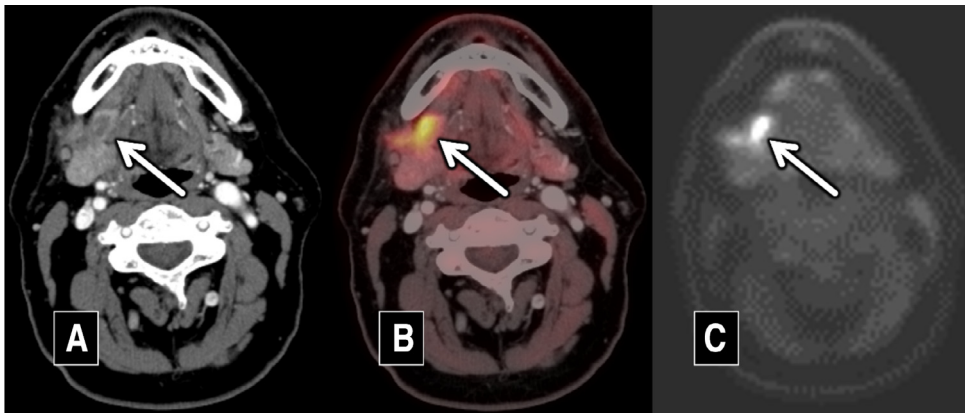

Figure 11 A 55-year-old man with right submandibular gland mass shown on axial postcontrasted standard algorithm CT (A, arrow), correlating axial fused FDG-PET/CT (B, arrow), and axial PET (C, arrow). Upon exploration, this was found to be squamous cell carcinoma from adjacent mucosal disease invading the submandibular gland.

adults, the vast majority of parotid gland tumors are benign in etiology. Of note, pleomorphic adenoma accounts for 65% of all parotid gland tumors. Interestingly, an inverse relationship exists for salivary gland size and incidence of malignant neoplasms.The incidence of primary epithelial salivary gland malignancy in the parotid, submandibular, sublingual, and minor salivary glands are 30%, 40%, 90%, and 50%, respectively.[1,4] Infrequently, there can also be invasion of salivary glands by adjacent aggressive neoplasms, which can be better evaluated with FDG-PET imaging (Figs. 11 and 12).

Perineural Tumor Spread

When evaluating malignant salivary gland neoplasms, particularly adenoid cystic carcinoma, the diagnostic radiologist must closely evaluate for evidence of perineural tumor spread, as this portends a poor prognosis.[9] Intracranial spread of tumor along the cranial nerves may result in alteration of surgical approach or an alternative treatment approach altogether. Linear areas of FDG avidity along the expected course of one or more cranial nerves are highly suspicious for perineural tumor spread. Given the superior tissue contrast resolution of MRI relative to CT, FDG-PET/MRI may serve as a particularly attractive tool for evaluating perineural tumor spread compared to FDG-PET/CT (Fig. 13). Unfortunately, the availability of hybrid PET/MRI systems is currently limited in the United States, therefore limiting the practicality of this new imaging modality for the commonplace clinical evaluation of patients with suspected perineural tumor spread.

Predicting Post-Treatment Outcomes

Post-treatment imaging of salivary gland malignancies following chemotherapy and/or radiotherapy should be delayed 6-8 weeks after cessation of therapy to prevent confusion of FDG-avid post-treatment changes with that of residual/recurrent tumor. Several small studies have shown potential advantages of FDG-PET imaging when it comes to predicting

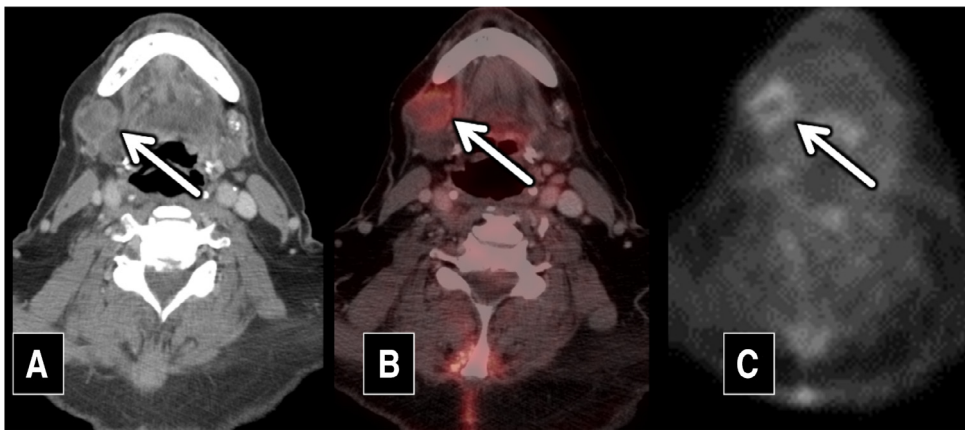

Figure 12 Submandibular gland mucoepidermoid carcinoma. Axial postcontrasted standard algorithm CT (A), correlating axial fused FDG-PET/CT (B), and axial PET (C) demonstrate a low density (A, arrow) lesion within the right submandibular gland with subtle peripheral increased FDG uptake (B and C, arrows), which was found to be a mucoepidermoid carcinoma on biopsy.

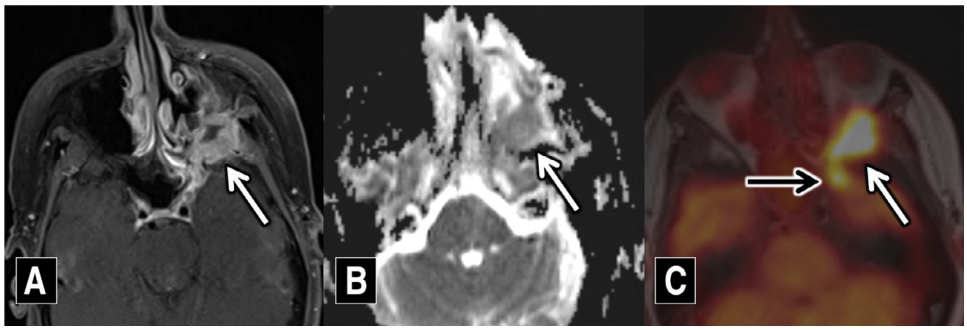

Figure 13 FDG-PET/MRI for assessment of perineural tumor spread. Axial T1-weighted (T1WI) postcontrast fat-saturated MRI (A) in a patient with squamous cell carcinoma shows invasion of the infrazygomatic masticator space (white arrow) and pterygopalatine fossa. Axial ADC map (B) shows reduced diffusivity of the tumor (white arrow), indicating high cellularity. Axial fused FDG-PET/MRI T1WI (C) shows the mass to have marked FDG avidity (white arrow). Note linear FDG uptake (black arrow) corresponding with perineural tumor spread along cranial nerve V2.

disease response to radiotherapy. For example, salivary gland carcinoma, a particularly aggressive primary salivary gland tumor, with higher SUV values (greater than or equal to 7.4) is associated with lower rates of recurrence and improved overall survival rates.[10] Interestingly, from a preoperative perspective, higher background metabolic rates (based on SUV values) within the parotid glands has been shown to correspond with lower risk of xerostomia following radiotherapy of head and neck neoplasms.[11]

Other Salivary Gland Pathology

Elevated FDG uptake within the parotid and submandibular glands has been documented in the setting of IgG4 sclerosing sialadenitis, with up to 98% of patients demonstrating elevated submandibular gland uptake and 35% within the parotid glands. There is also a propensity for this disease to demonstrate bilaterality with up to 89% of patients showing bilateral submandibular gland uptake. Other pathologies such as dendritic (Langerhans) cell histiocytosis may also show bilateral impressive increased uptake of the salivary glands on FDG-PET imaging (Fig. 14).

Conclusion

While traditional cross section imaging with CT and MRI are often utilized for evaluating salivary gland malignancy, FDG-PET/CT and FDG-PET/MR imaging can assist with lesion evaluation. Recent publications have demonstrated the power of diffusion weighted imaging apparent diffusion coefficient values as a rough marker of cellularity for pathologies throughout the head and neck (Fig. 13), but FDG-PET imaging has been found most useful in whole body evaluation for salivary gland malignancies to distant sites, as well as distant primary metastases to the salivary glands (Figs 15 and 16). Although there is a paucity of published literature on the use of FDG-PET imaging for salivary gland tumors relative to other primary malignancies within the head and neck, there are common clinical circumstances when FDG-PET imaging can greatly assist in these complex patients, potentially significantly changing therapy.

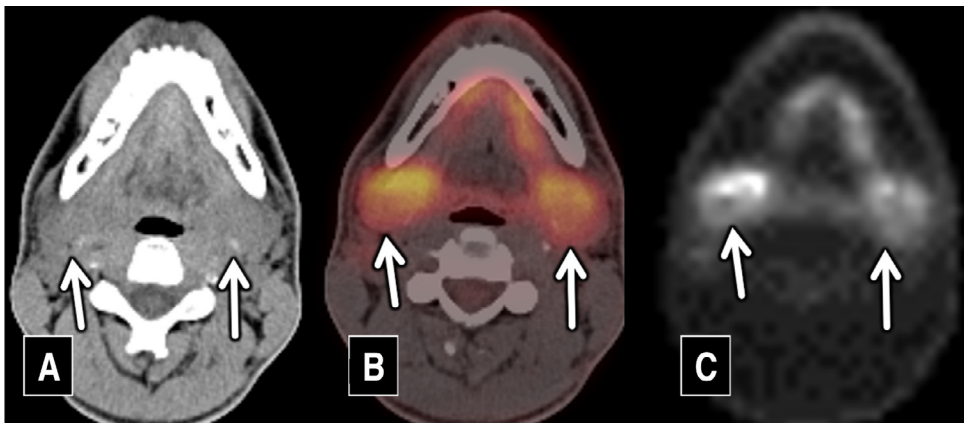

Figure 14 A 20-year-old patient with biopsy-proven dendritic (Langerhans) cell histiocytosis of the submandibular glands. Axial noncontrast CT (A) shows bilateral enlargement of the submandibular glands (white arrows) with correlating increased uptake on axial fused FDG-PET/CT (B, arrows) and axial PET (C, arrows).

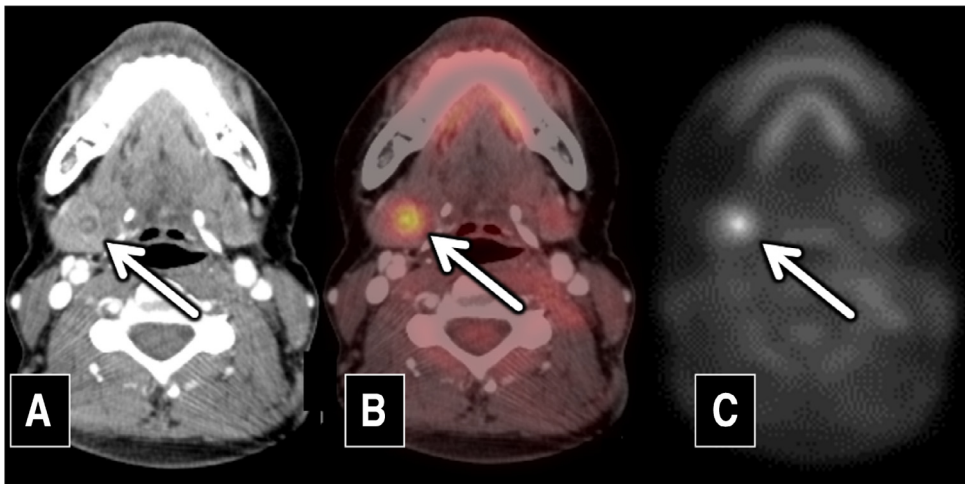

Figure 15 A 30-year-old woman with a right submandibular gland mass (arrows) seen on axial postcontrasted standard algorithm CT (A) and correlating increased uptake on axial fused FDG-PET/CT (B) and axial FDG-PET (C), found to be adenoid cystic carcinoma on biopsy.

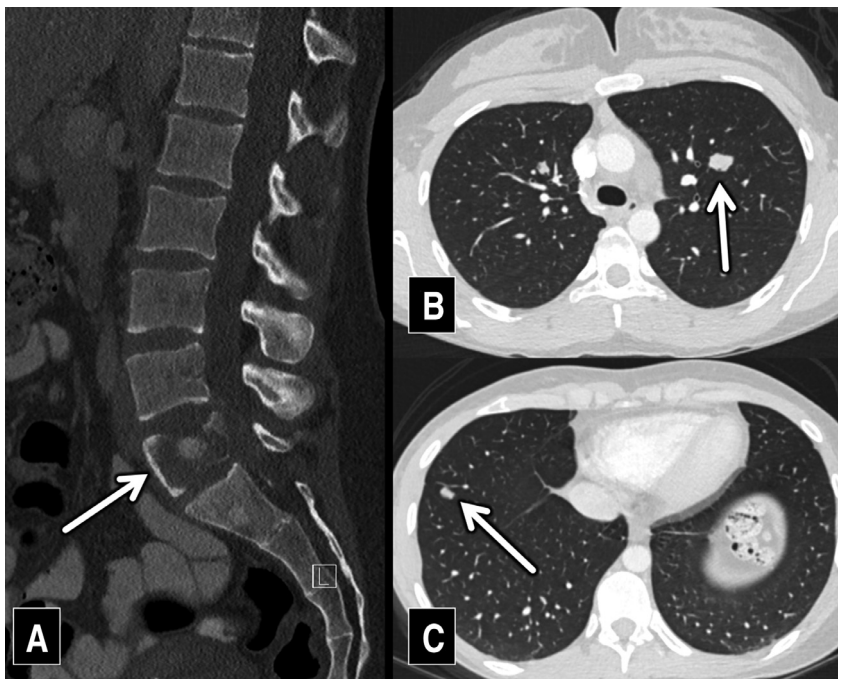

Figure 16 Distant metastatic disease found in the same patient as Figure 15 with sagittal bone algorithm CT reconstruction demonstrating a vertebral body metastatic focus (A, arrow), and bilateral lung metastatic disease found on axial lung algorithm windows (B and C, arrows).

References

1. Guzzo M, Locati LD, Prott FJ, et al: Major and minor salivary gland tumors. Crit Rev Oncol Hematol 74:134-148, 2010
2. Francis Thottian AG, Gandhi AK, Ramateke PP, et al: Acinic cell carcinoma of parotid gland with cavernous sinus metastasis: A case report. J Cancer Res Ther 14:1428-1430, 2018
3. Lee SH, Roh JL, Kim JS, et al: Detection of distant metastasis and prognostic prediction of recurrent salivary gland carcinomas using 18 F-FDG PET/CT. Oral Dis 24:940-947, 2018
4. Freling N, Crippa F, Maroldi R: Staging and follow-up of high-grade malignant salivary gland tumours: The role of traditional versus functional imaging approaches—A review. Oral Oncol 60:157-166, 2016
5. Haberal MA, Akar E, Dikis OS: Metastatic lung cancer associated with Warthin's tumour. Niger J Clin Pract 22:585-587, 2019
6. Bradley PJ, Mcgurk M: Incidence of salivary gland neoplasms in a defined UK population. Br J Oral Maxillofac Surg 51:399-403, 2013
7. Makis W, Ciarallo A, Gotra A: Clinical significance of parotid gland incidentalomas on (18)F-FDG PET/CT. Clin Imaging 39:667-671, 2015
8. Seo YL, Yoon DY, Baek S, et al: Incidental focal FDG uptake in the parotid glands on PET/CT in patients with head and neck malignancy. Eur Radiol 25:171-177, 2015
9. Paes FM, Singer AD, Checkver AN, et al: Perineural spread in head and neck malignancies: Clinical significance and evaluation with 18F-FDG PET/CT. Radiographics 33:1717-1736, 2013

10. Hsieh CE, KC Ho, Hsieh CH, et al: Pretreatment primary tumor SUVmax on 18F-FDG PET/CT images predicts outcomes in patients with salivary gland carcinoma treated with definitive intensity-modulated radiation therapy. Clin Nucl Med 42:655-662, 2017 Sep

11. Van dijk LV, Noordzij W, Brouwer CL, et al: F-FDG PET image biomarkers improve prediction of late radiation-induced xerostomia. Radiother Oncol 126:89-95, 2018